



HAL
open science

Robotic optical-micromanipulation platform for teleoperated single-cell manipulation

Edison Gerena, Florent Legendre, Youen Vitry, Stephane Regnier, Sinan Haliyo

► **To cite this version:**

Edison Gerena, Florent Legendre, Youen Vitry, Stephane Regnier, Sinan Haliyo. Robotic optical-micromanipulation platform for teleoperated single-cell manipulation. 2019 International Conference on Manipulation, Automation and Robotics at Small Scales (MARSS 2019), 2019, Helsinki, Finland. pp.60, 10.1109/MARSS.2019.8860946 . hal-03190968

HAL Id: hal-03190968

<https://hal.science/hal-03190968>

Submitted on 29 Aug 2023

HAL is a multi-disciplinary open access archive for the deposit and dissemination of scientific research documents, whether they are published or not. The documents may come from teaching and research institutions in France or abroad, or from public or private research centers.

L'archive ouverte pluridisciplinaire **HAL**, est destinée au dépôt et à la diffusion de documents scientifiques de niveau recherche, publiés ou non, émanant des établissements d'enseignement et de recherche français ou étrangers, des laboratoires publics ou privés.

Robotic Optical-micromanipulation Platform for Teleoperated Single-Cell Manipulation

Edison Gerena¹, Florent Legendre¹, Youen Vitry², Stéphane Régnier¹ and Sinan Haliyo¹

Abstract—Single cell manipulation is considered a key technique for biological application. However, the lack of intuitive and effective systems make this techniques less widespread. We propose here a new tele-robotic solution for dexterous cell manipulation through optical tweezers. The slave robot consist in a combination of robot-assisted stages and a high-speed multi-trap technique and allows the manipulation of more than 15 optical traps in a workspace of $(200 \times 200 \times 200) \mu\text{m}^3$ for translations and $(70 \times 50 \times 8) \mu\text{m}^3$ for rotations, both with nanometric resolution. The master device with 6+1 Dof is employed to control the 3D position of optical traps in different arrangements. Traps can be grouped and controlled in a variety of ways for specific purposes. Precision and efficiency studies are carried out with trajectory control tasks. Finally, the 6D teleoperated-control of an optical robot for cell-transport is presented. Results exemplify the kind of biological applications that can be accomplished with the presented system in an effective and intuitive way, even if the user does not come from an engineering background.

I. INTRODUCTION

Dexterous manipulation of single-cells offers many possible applications in cellular surgery, cell mechanobiology, tissue engineering and biophysics, among others. Recent breakthrough in biotechnology are creating a rising demand for complex single-cell operation techniques such as cell isolation, 3D orientation and cell-injection. Nowadays, those tasks are usually performed using simple 3-axes cartesian robots. Most of commercial solutions consist of motor-driven micromanipulators composed of prismatic joints and micropipettes or microgrippers as end-effectors. Controlled through buttons or knobs, those systems are not ergonomic and require an experienced operator to be used. The realization of basic tasks, like the rotation of a cell, proves to be time-consuming and challenging due to the lack of dexterity brought by those control interfaces.

Single-cell manipulation still presents significant challenges mainly due to the physics involved (volumetric forces dominated by the surfaces forces) and the size limitations imposed by the environment. The resolution and precision required at those sizes have a cost in term of Degree-of-Freedom, working space, grasping strategies and control schemes. In addition, the demand for

manipulation in confined environments like micro-fluidic devices is increasing, in order to reduce external perturbation and contamination of the study sample. However this type of environment is unreachable by conventional manipulators.

To address those issues, several approaches for actuated untethered micro-robots have been proposed by chemical reactions, physical fields or bio-hybrid approaches [1]. Remote actuation of micro-robots using external fields as magnetic, acoustic, electrostatic or optical has appear as very promising solutions. Among them, optical trapping present diverse advantages in the manipulation of small biological samples.

Optical trapping exploits the pressure of radiation to trap suspended micro-objects in a fluid. It allows indirect manipulation with nanometer precision in confined spaces resulting in contamination-free and contact-free method for cell manipulation in their culture medium. Furthermore, it is possible to trap simultaneous several objects using a unique laser source by active diffractive optical elements (Holographic Optical Tweezers) [2] or by rapid laser-deflection (Time-shared methods) [3]. In contrast to others techniques using magnetic or acoustic fields, the high spacial resolution of optical trapping allows the direct implementation of collaborative task by several trapped objects. Ultimately, using optical-robots (i.e. 3D-printed micro-structures controlled by optical-trapping), it is possible to indirectly manipulate cells in order to avoid biological damage that might be inflicted by direct laser exposition. Physical and chemical treatments in optical-robot manufacturing also allow the specialization of the robots for more specific tasks such as ph sensor [4], temperature sensor [5] or puncturing of cells [6].

Fully automated control at micro-scale is still challenging, since the studied samples are, most of the time, unstructured and the environment variables uncertain. Furthermore, because the design of the optical robots can be done specifically for a given requirements in a particular experiment, the system needs to be able to adapt to any type of printed structure. Proposing a complete automated implementation for each situation will be inefficient, as most of the protocols are not completely defined before the operation. In addition, automatizing a particular task is often outside of the end-user competences.

Macro-manipulation research has addressed similar issues through control by teleoperation. In this case, the operator controls the robot manipulator (slave device) using an other robot (master device), which allows to keep human intelli-

*This work was supported by the French National Research Agency through the ANR-IOTA project (ANR-16-CE33-0002-01), and partially by the French government research program "Investissements d'avenir" through the Robotex Equipment of Excellence (ANR-10-EQPX-44).

¹Authors are with Sorbonne Université, CNRS, Institut des Systèmes Intelligents et de Robotique, ISIR, F-75005 Paris, France.

²Y. Vitry are with Université libre de Bruxelles, BEAMS dpt, CP 165/56, 50 avenue Roosevelt, B-1050 Brussels.

(Correspondence e-mail: edison.gerena@isir.upmc.fr)

gence in the loop and benefit from the user know-how and its ability to adapt the protocol according to the external perturbation or the particularity of the task. A good example is the Da Vinci System (Intuitive Surgical, Inc), designed to facilitate complicated minimally invasive surgery by accurately scaled the macroscopic movements of the hand from the surgeon console to an endoscopic wrist placed within the chest cavity of the patient. Teleoperation systems have already been successfully implemented in several domains such as robotic surgery, under-water vehicles or nuclear robots.

Existing commercial interfaces for optical manipulation allow the user to control the optical traps using 2D mouse position. In order to enhance the user control, some attempts to incorporate more efficient master devices have been made, such as joysticks [7], gesture recognition (e.g. 2D cameras, Kinect, Leap-motion) [8], [9], [10], multi-touch tablets [11], [12] and 3D robotised interfaces (or haptic interface) [13], [14], [15]. Some deeper multi-modal methods have been attempted using combinations of gesture recognition, eye gaze tracking or speech recognition [16], [17].

Despite the improvement brought by those attempts in terms of ergonomics and efficiency, the realization of complex tasks continues to be challenging. Mouses, joysticks and tablets do not permit to apprehend a three-dimensional workspace. Tracking sensors suffer from lack of resolution in temporal and spatial dimensions. 3D robotised interfaces were used to control only one object at a time. In addition, multi-trap actuation techniques used in most of these platforms are based on Spatial Light Modulators (SLM), which provide limitations by adding a time latency in the control-loop resulting from the reactivity of their hardware and a high calculation cost for a given trajectory.

Because of the high dynamic phenomena occurring in the micro-world, a reliable 3D real-time micro-manipulator needs a spatial and temporal resolution compatible with these effects, making the performance of the optical set-up and the coupling between master and slave devices critical parts. Based on all these observations, we presented a teleoperated optical micro-manipulator platform for direct and indirect single-cell dexterous manipulation.

The system is based on optical actuation allowing a non-contact manipulation of biological samples or micro-machines. The working space is optimized by combining a 3D multi-trap time-shared method, a 3D nano-stage and a 2D micro-stage. In order to reduce the latency issue in the hardware, the 3D multi-trap technique is based on a high-bandwidth steering mirror and a deformable mirror [18]. The teleoperation is realized via a master device (Omega.7) providing 6+1 DoF and the master/slave coupling is ensured by a hard real-time system. The performances of the system in terms of static and dynamic precision are evaluated using trajectory control tasks. Finally, 6D teleoperation control of an optical robot is demonstrated during a cell-transportation experiment. The results exemplify the kind of biological applications that can be accomplished in an effective and intuitive way with the proposed platform.

II. TELEOPERATION SYSTEM DESIGN

A. Optical System

The system is constructed around an inverted microscope (Oil immersion, Olympus UPlanFLN 40x, NA 1.3). The same objective is used for imaging the sample and to generate the optical-traps. The source is chosen as a Near-infrared Laser (1070 nm) to minimize the photo-damage in biological objects. The beam is expanded in order to overfill (20%) the objective entrance to improve the trapping efficiency [19]. The illumination (LED, 3 W) is reflected by a longpass dichroic mirror into a High-Speed CMOS camera (Basler, 659×494 pixels) in order to provide visual perception to the operator.

B. High-Bandwidth 3D Multi-Trap Actuation

In order to generate simultaneously several optical traps, the laser is regularly deflected between the different wanted trap positions using a 2D mirror galvanometer (GVS002, Thorlabs) and a deformable mirror (PTT111 DM, Iris AO). This time sharing method is made possible by the high reactivity of the galvanometer and the deformable mirror, and a hard-real time control framework implemented in C++ on a Real-Time kernel (Xenomai).

This design allows the creation of numerous independent optical traps within a volume of approximately $70 \times 50 \times 8 \mu\text{m}^3$ with a bandwidth up to 200Hz.

The deformable mirror can handle a 1kHz sampling rate for Z axis displacement below $2 \mu\text{m}$. In order to use the full range available of $7 \mu\text{m}$, the control loop frequency is fixed at 200Hz. Controlled in open-loop, the deformable mirror needs to be calibrated to provide the best performances.

The galvanometer has comparable capacities with a bandwidth from 250Hz to 1kHz for angles below 0.2° . The galvanometer is controlled in closed-loop and has a specified angular resolution of 0.0008° . For further details please see [18].

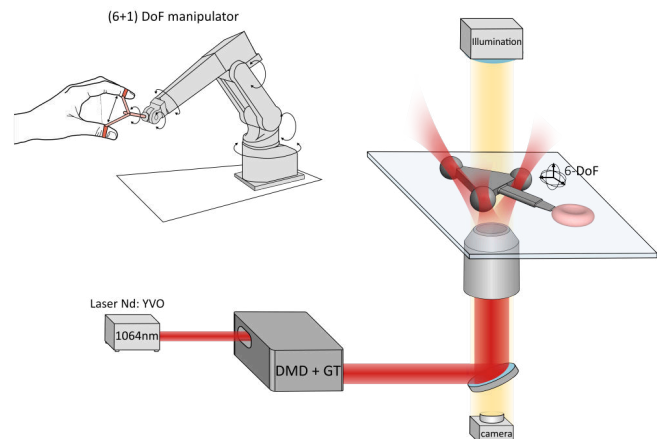


Fig. 1. The overall system scheme. Three main parts make up the platform: Master Device (7 DoF Robot Manipulator), Optical set-up (Laser + optical instruments) and the Slave robot (robot-assisted stages and 3D multi-trap actuator). The Slave robot can be used directly or indirectly (i.e. through beads or optical robots) manipulated single-cells.

TABLE I
SUMMARY OF THE PLATFORM PARAMETERS

Translation range	$200 \times 200 \times 200 \mu\text{m}^3$
Rotation range	$70 \times 50 \times 8 \mu\text{m}^3$
Rotation full scale bandwidth	200 Hz
Rotation small scale ($\pm 2 \mu\text{m}$ in z) bandwidth	2 KHz
Teleoperation loop	200 Hz
Stable independent optical traps	> 15
Optical loss	< 3%

C. Master-Slave Control

Made for teleoperation, the system is build as an open-loop Master-Slave system. The Master device is a Omega (Omega.7, ForceDimension), which allow 7 Degree of Freedom (DoF) control of the Slaves (robot-assisted stages handling the sample and traps positions). On the 7 DoF, 3 DoF are for translations, 3 DoF are for rotations and a last DoF are for translations, 3 DoF are for rotations and a last DoF is given by a gripper under the index finger of the user.

Two different types of actuation coexist to control the motion of optical traps. The first one is composed of a 3D nano-stage mounted on a 2D micro-stage. The micro-stage allows to evolve in the complete workspace (petri dish: $25 \times 25 \text{mm}^2$), while the nano-stage gives a finer control in a $200 \times 200 \times 200 \mu\text{m}^3$ range. The second type is composed of the galvanometer and the deformable mirror (see High-Bandwidth 3D Multi-Trap Actuation section). High-speed laser deflection allow the creation of several optical traps and positioned in a 3D working-space of $70 \times 50 \times 8 \mu\text{m}^2$ limited by the field-of-view (FoV) of the camera for planar motions, and the actuator range for axial motion.

The processed sample is placed on the nano-stage. The nano-stage and the micro-stage are directly moving the sample, which creates a translation of the surroundings while optical traps maintain the manipulated object fixed to the field-of-view.

The master device position is converted in a translation command sent to the nano-stage. The master device orientation is used to compute a rotation matrix which will indicate the new positions of the traps to the galvanometer and the deformable mirror. Finally, the gripper position is interpreted to determine new traps positions depending on this operating.

The gripper has two operating modes. The 'Radial' mode moves the wanted traps toward or away from the rotation center. This type of radial motion allow the user to grasp something using little objects as 'fingers'. The 'Scissor' mode rotates the wanted traps towards the Y axis in order to give a 'scissor like' movement to a set of traps. It can be used to actuate tools like clamps.

From the user point of view, the optical traps can be dynamically created via the control interface. The number of traps is not limited, but their stiffness decrease with their number. Each trap coordinate can be directly edited on the fly. The optical traps can be organized by groups. For each group, the rotations and the gripper functionality can be independently enabled or disabled. Fig. 2 shows

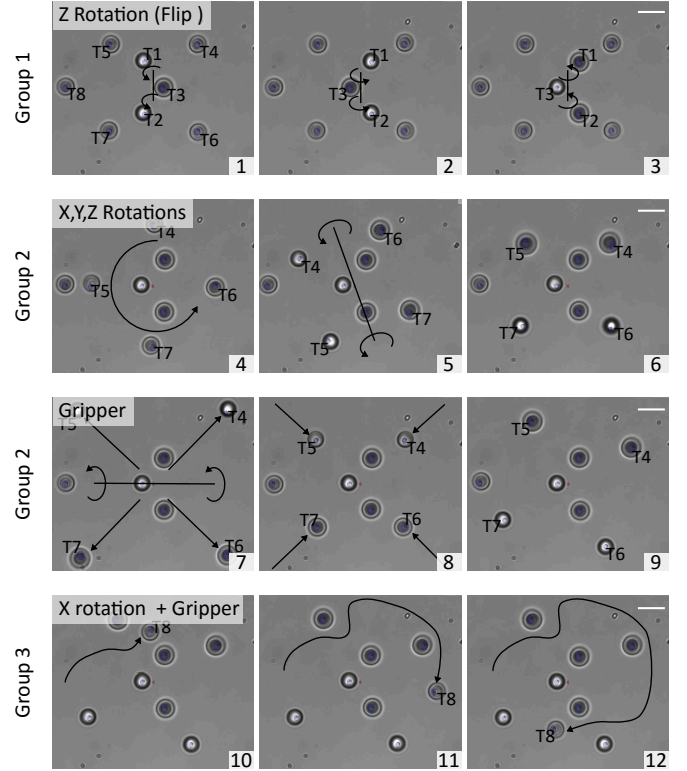


Fig. 2. Example of 3D teleoperation using 3 groups of traps. The operation is a succession of four different tasks demonstrating the system capacity. The first task (Pictures 1, 2 and 3) is a 3D reversal around the Z axis of a micro-beads triangle. The second task (Picture 4, 5 and 6) show the 3D control of a four micro-beads square. The third task (Picture 7, 8 and 9) present the 'Radial' operating mode of the gripper. Finally, the last task (Picture 10, 11 and 12) present the travel of one micro-bead around all the others locked in rotation. Scale bars are $5 \mu\text{m}$ long.

an example of 3D teleoperation using several groups of traps. The translation and rotation actuators have two control modes, the Position mode and the Velocity mode:

1) *Position mode*: This first mode mirrors the master device position and orientation to the slaves to make the control as transparent as possible for the user and give the feeling to directly hold the trapped object in the hand.

2) *Velocity mode*: This second mode permits to control the velocity of the slaves. The motion direction and amplitude is computed according to the vector made by the center of the master device workspace and the position of the handle. The velocity control mode can be enabled independently for the translations and rotations.

III. CHARACTERIZATION OF THE SYSTEM

In order to evaluate the system performances, the data from the master device, the command sent to the actuators and the video from the camera are recorded during the teleoperation. The video is then processed afterwards to determine the trapped object real position. For each recorded data, the current system time is added for synchronization purposes.

Due to their actuation method, translations relocation the complete FoV, rendering the position shift arduous to eval-

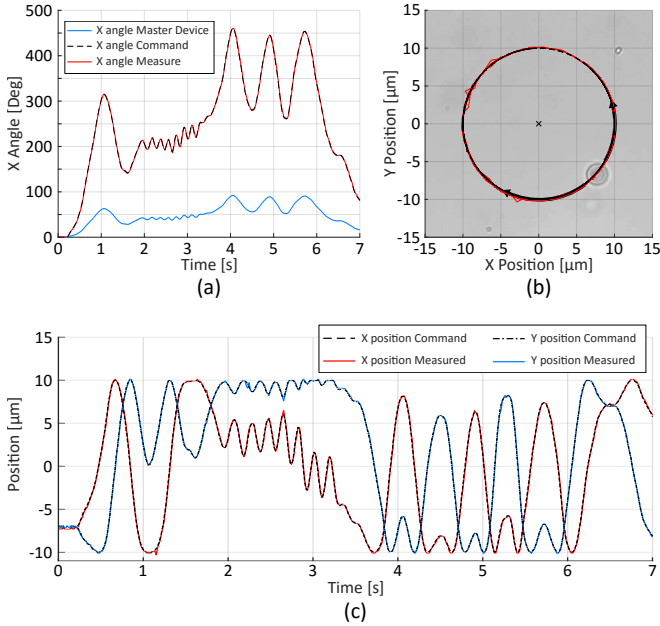


Fig. 3. Example of teleoperated rotation in position mode of a trapped micro-bead; (a) The master device orientation is used to compute the optical trap position. The actual angle is estimated from the measured trap position; (b) Trajectory of the micro-bead. During the experience, the micro-beads rotate around the marked center; (c) Position command sent to the mirrors and measured position computed from the video.

uate. Furthermore, the camera tracking does not allow to estimate depth, so only 2D rotational motion induced by the galvanometer and the deformable mirror are studied.

A. Static precision

The optical trap stiffness determines the stability of the trapped object. Since the traps are generated by laser time sharing, the stiffness of each trap decreases with their number and makes the trapped object more sensitive to external forces like Brownian motion and viscosity forces.

The static precision depends on the actuators accuracy and Brownian motion which in turn is trap-stiffness and temperature dependent. To evaluate those two parameters combined, 13 micro-beads were trapped and positioned to

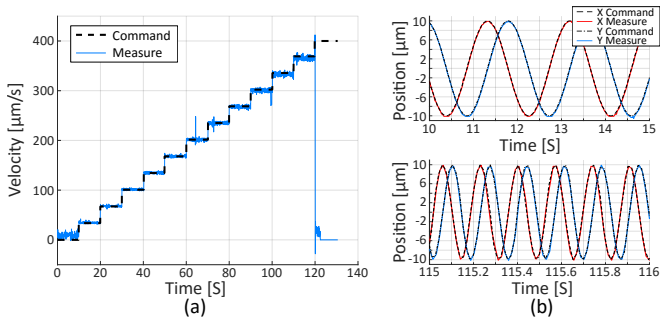


Fig. 4. Example of teleoperated rotation in velocity mode of a trapped micro-bead. The handle orientation of the master device is locked to generate speed step using the adjustable command gain; (a) The set velocity and the measured velocity calculate from the measured bead positions; (b) The bead position follow the command at low and high velocity.

cover a $20 \times 20 \mu\text{m}$ square as shown in Fig. 5. The data were recorded during 15s. The variation of the measured positions inform about the stability and the average compared to the commands deliver the local static precision. The results indicates an overall precision of $1 \mu\text{m}$.

B. Dynamic precision

To measure the dynamic precision, a micro-bead is trapped and rotated at different velocities around a reference point. The result, shown in Fig. 4, confirm a correct tracking of the command in velocity mode up to $380 \mu\text{m/s}$. The same experiment done with 4 trapped micro-beads, shown in Fig 6, demonstrates also a proper tracking of the command.

Two interesting differences can be noticed between the two experiments. On first hand, the highest reachable velocity is lower when 4 micro-beads are trapped. The reason hides in the actuation method. The laser is deflected at a constant frequency of 200Hz from one trap to another, meaning that the motion induced by changing those trap positions is not linear. The position is moved by step and the higher the velocity of the motion is, the larger the position steps are.

As the multi-trap actuation is based in a time-sharing method, the distance between two position is given by the following equation:

$$D_{pos} = \frac{V}{f} \quad (1)$$

Where D_{pos} is the distance between two different position of the same trap, V the velocity of the motion and f the deflecting frequency of the laser (200Hz). The highest velocity reached is roughly $400 \mu\text{m/s}$ for 1 trap and $100 \mu\text{m/s}$ for 4 traps. For both experiences, this velocity correspond to a gap of $2 \mu\text{m}$ between two consecutive positions of a same trap. Considering the $3 \mu\text{m}$ diameter of the micro-beads, $2 \mu\text{m}$ can define the limit before losing the trapped object. This result is similar to literature, as the linearity of the trap stiffness is valid around one radius of the trapped bead [20], here $1.5 \mu\text{m}$. Note that the highest velocity is defined at the edges of the trap.

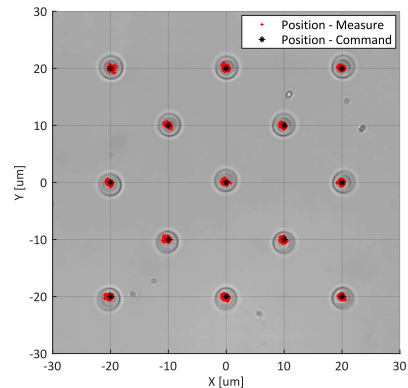


Fig. 5. Position during 15s of 13 micro-beads set to cover a $20 \times 20 \mu\text{m}$ square. The maximum error between the command and the actual position reaches $1 \mu\text{m}$ and is essentially due to Brownian motion.

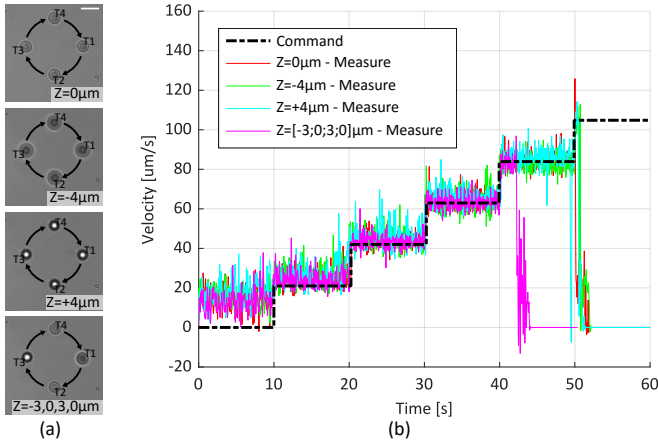


Fig. 6. Example of teleoperated rotation in velocity mode of 4 micro-beads at different Z positions. The handle orientation of the master device is locked to generate speed steps using the adjustable command gain; (a) 4 different configurations. Scale bar is $5\mu\text{m}$ long; (b) The measured velocity calculated from the video and the command sent to the mirrors.

Based on those observations, the following equation predicts the theoretical highest reachable velocity depending on the number of optical traps generated and the deflecting frequency of the laser:

$$V_{max} = \frac{D_{max} * f}{N_{trap}} \quad (2)$$

V_{max} is the maximum stable velocity, D_{max} the maximal stable distance between two different position of the same trap ($2\mu\text{m}$), N_{trap} the number of optical traps generated and f the deflecting frequency of the laser (200Hz). As a consequence, if the deflecting frequency of the laser is set to a higher value, the maximum reachable velocity increases.

On second hand, the velocity measured is more noisy when the 4 micro-beads are trapped. The stiffness of the traps decreases with their number and the high-frequency noise observed is the result of the bigger Brownian motion on the less stiff traps.

As said before, an object can be lost if the distance between the center of the object and the optical trap is larger than $2\mu\text{m}$. This gap can be reached by different ways depending on the actuation method in action. When the translation actuators are used, the viscosity in the environment applies a force on the trapped object depending on the motion velocity. When only one trap is created, the impact of the viscosity is small. The maximum velocity measured without losing the object is $1100\mu\text{m/s}$. When several traps are generated, the object are not constantly trapped and the viscosity will have a much stronger effect. During the time period when the trap is not active, the viscous force will push the object out of the trap and the object might be lost if the velocity is too high. For 4 traps created, the maximum translation velocity measured without losing the object is $110\mu\text{m/s}$.

IV. EXPERIMENT ON BIOLOGICAL SAMPLE

To illustrate the kind of biological applications that can be accomplished with the proposed platform in a real world

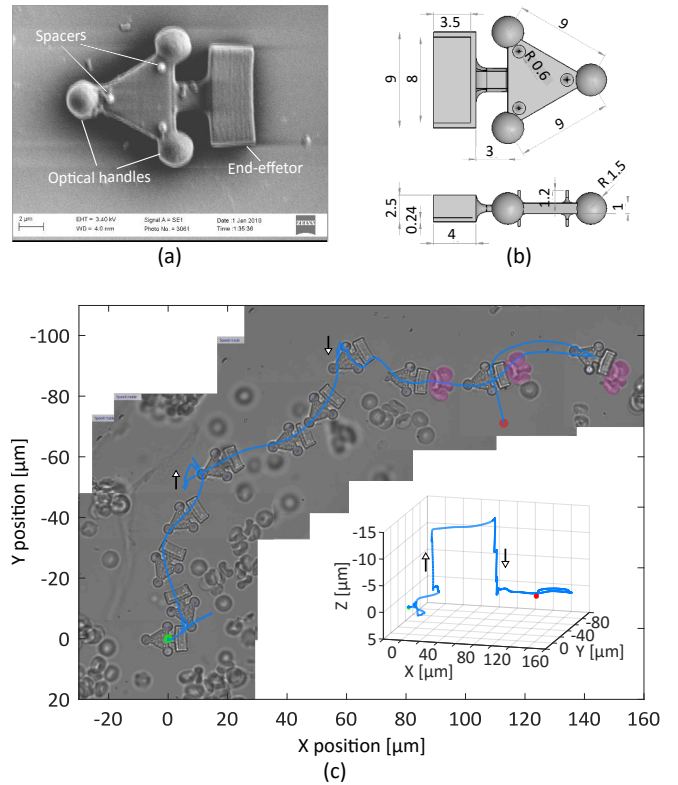


Fig. 7. (a) Scanning electron microscopy (SEM) image of the robot; (b) Schematic depictions with dimensions of optical robot. Dimensions are in micro-meters; (c) Trajectory of the teleoperated Robot. Blue line is the 3D trajectory of the robot. Arrows shows the moments where the robot is elevated and lowered in the Z-direction. Note that frames between the arrows shows the RBC cells out-of-focus because the focus is made on the robot. Finally a cluster of cell (colored in violet) is transported on $80\mu\text{m}$.

scenario, Red-Blood Cells (RBC) are selected as manipulated objects. Several studies have shown that direct cell trapping can cause considerable photo-damage and even induce the death of cells [21], [22]. Therefore, we chose to indirectly manipulate the cells through an optical robot.

This type of manipulation is a good illustration of the capabilities and versatility of the system. Unlike the manipulation of individual beads, during manipulation of rigidly linked structures, the positions errors of each trap and any synchronization problem in the movements of groups will affect the stability of the whole structure. Hence, controlling the 3D movement of an optical robot is a demanding task.

A. Fabrication and collection of the Robot

As at least three handles are necessary to induce complete spatial motion, an optical robot with three spherical handles has been designed. The micro-robot is manufactured according to the dimension specifications shown in Fig. 7.(b), by two-photon polymerization (2PP) (Nanoscribe Photonic Professional) using IP-Dip resin (refractive index ~ 1.52). The robot has a shovel-shaped end-effector, in order to push and move several cells at the same time. Different spacers are attached on both sides of the robot to minimize the adhesion forces. See Fig. 7.(a).

After fabrication, the robots are incubated in a 94.5% distilled water, 5% ethanol and 0.5% *Tween20* solution to prevent the surface adhesion. For experiments, micro-robots are transferred to a sample chamber containing suspended RBC through an actuated syringe (Hamilton, 250 μL). Then, the sample chamber is sealed with a cover-slip.

B. Teleoperated Optical Robot for cell transportation

Once transported, the optical robot is controlled using our developed platform. A group of three traps in a triangle configuration is generated using the user interface. Then, teleoperation of the traps are performed through the Master device allowing 6-Dof motion of the optical-robot.

Thanks to the low response-time and transparency of the system, the operator manages to open a path through a sample heavily loaded in suspended RBC. Fig. 7(c) shows the trajectory of the teleoperated Robot. At the beginning the robot is in the bottom of the Petri-dish. Then, the robot is elevated in the Z-direction (10 μm) as the obstacles completely blocks the path. Once the target cells are identified, the axial position of the robot is decreased until they hit again the bottom. Finally, the robot move indirectly the cluster of cells for 80 μm .

The experiment illustrates the kind of application where our developed platform can be implemented for single-cell manipulations. Possible applications include pushing, rotating biological samples, avoiding obstacles, exploring, sensing 3D samples and for any dexterous cell handling purposes.

V. CONCLUSION

We have presented a new platform for dexterous cell handling through optical manipulation. As a result of efficient architecture the dexterous manipulation of more than 15 optical traps in a working space of (70 \times 50 \times 8) μm^3 for rotations and (200 \times 200 \times 200) μm^3 for translations with nanometric resolution is presented. The characterization of the system shows a static precision of less than 1 μm for the manipulation of 13 simultaneously trapped objects. Concerning the dynamic motion, a maximal handling velocity has been defined according to the number of traps, in order to assist the user and ensure the retention of the trapped objects.

The system provides a straightforward human/machine interaction bringing the optical manipulation to a new level of usability and allowing users to take advantage of its full potential, even if the user does not come from an engineering background. Complex arrangements of optical traps can be grouped and transformed in a variety of ways to achieve diverse tasks. Thanks to the capabilities of the system, and because of the stable and simple set-up design, concrete task have been demonstrated in a real biological environment. This is a good illustration of the kind of new biological application that can benefit from the proposed platform. Earlier experiment on cell indicates that the platform may provide a powerful tool for cell sorting, manipulation, stimulation and assembling.

REFERENCES

- [1] H. Ceylan, J. Giltinan, K. Kozielski, and M. Sitti, "Mobile microrobots for bioengineering applications," *Lab on a Chip*, vol. 17, no. 10, pp. 1705–1724, 2017.
- [2] J. E. Curtis, B. A. Koss, and D. G. Grier, "Dynamic holographic optical tweezers," *Optics communications*, vol. 207, no. 1-6, pp. 169–175, 2002.
- [3] F. Arai, K. Yoshikawa, T. Sakami, and T. Fukuda, "Synchronized laser micromanipulation of multiple targets along each trajectory by single laser," *Applied Physics Letters*, vol. 85, no. 19, pp. 4301–4303, 2004.
- [4] H. Maruyama, T. Fukuda, and F. Arai, "Functional gel-microbead manipulated by optical tweezers for local environment measurement in microchip," *Microfluidics and Nanofluidics*, vol. 6, no. 3, p. 383, 2009.
- [5] S. Fukada, K. Onda, H. Maruyama, T. Masuda, and F. Arai, "3d fabrication and manipulation of hybrid nanorobots by laser," in *Robotics and Automation (ICRA), 2013 IEEE International Conference on*. IEEE, 2013, pp. 2594–2599.
- [6] T. Hayakawa, S. Fukada, and F. Arai, "Fabrication of an on-chip nanorobot integrating functional nanomaterials for single-cell punctures," *IEEE Transactions on Robotics*, vol. 30, no. 1, pp. 59–67, 2014.
- [7] G. Gibson, L. Barron, F. Beck, G. Whyte, and M. Padgett, "Optically controlled grippers for manipulating micron-sized particles," *New Journal of Physics*, vol. 9, no. 1, p. 14, 2007.
- [8] C. McDonald, M. McPherson, C. McDougall, and D. McGloin, "Holo-hands: games console interface for controlling holographic optical manipulation," *Journal of Optics*, vol. 15, no. 3, p. 035708, 2013.
- [9] C. Muhiddin, D. Phillips, M. Miles, L. Picco, and D. Carberry, "Kinect 4 : holographic optical tweezers," *Journal of Optics*, vol. 15, no. 7, p. 075302, 2013.
- [10] L. Shaw, D. Preece, and H. Rubinsztein-Dunlop, "Kinect the dots: 3d control of optical tweezers," *Journal of Optics*, vol. 15, no. 7, p. 075303, 2013.
- [11] K. Onda and F. Arai, "Parallel teleoperation of holographic optical tweezers using multi-touch user interface," in *Robotics and Automation (ICRA), 2012 IEEE International Conference on*. IEEE, 2012, pp. 1069–1074.
- [12] R. Bowman, G. Gibson, D. Carberry, L. Picco, M. Miles, and M. Padgett, "itweezers: optical micromanipulation controlled by an apple ipad," *Journal of Optics*, vol. 13, no. 4, p. 044002, 2011.
- [13] K. Onda and F. Arai, "Robotic approach to multi-beam optical tweezers with computer generated hologram," in *Robotics and Automation (ICRA), 2011 IEEE International Conference on*. IEEE, 2011, pp. 1825–1830.
- [14] C. Pacoret and S. Régnier, "Invited article: A review of haptic optical tweezers for an interactive microworld exploration," *Review of Scientific Instruments*, vol. 84, no. 8, p. 081301, 2013.
- [15] M. Yin, E. Gerena, C. Pacoret, S. Haliyo, and S. Régnier, "High-bandwidth 3d force feedback optical tweezers for interactive bio-manipulation," in *Intelligent Robots and Systems (IROS), 2017 IEEE/RSJ International Conference on*. IEEE, 2017, pp. 1889–1894.
- [16] M. Grammatikopoulou and G.-Z. Yang, "Gaze contingent control for optical micromanipulation," in *Robotics and Automation (ICRA), 2017 IEEE International Conference on*. IEEE, 2017, pp. 5989–5995.
- [17] Z. Tomori, P. Keša, M. Nikorovič, J. Kaňka, P. Ják, M. Šerý, S. Bernatová, E. Valušová, M. Antalík, and P. Zemánek, "Holographic raman tweezers controlled by multi-modal natural user interface," *Journal of Optics*, vol. 18, no. 1, p. 015602, 2015.
- [18] E. Gerena, S. Regnier, and D. S. Haliyo, "High-bandwidth 3d multi-trap actuation technique for 6-dof real-time control of optical robots," *IEEE Robotics and Automation Letters*, 2019.
- [19] K. C. Neuman and S. M. Block, "Optical trapping," *Review of scientific instruments*, vol. 75, no. 9, pp. 2787–2809, 2004.
- [20] A. Ashkin, "Forces of a single-beam gradient laser trap on a dielectric sphere in the ray optics regime," *Biophysical journal*, vol. 61, no. 2, p. 569, 1992.
- [21] K. C. Neuman, E. H. Chadd, G. F. Liou, K. Bergman, and S. M. Block, "Characterization of photodamage to escherichia coli in optical traps," *Biophysical journal*, vol. 77, no. 5, pp. 2856–2863, 1999.
- [22] M. B. Rasmussen, L. B. Oddershede, and H. Siegmundfeldt, "Optical tweezers cause physiological damage to escherichia coli and listeria bacteria," *Appl. Environ. Microbiol.*, vol. 74, no. 8, pp. 2441–2446, 2008.